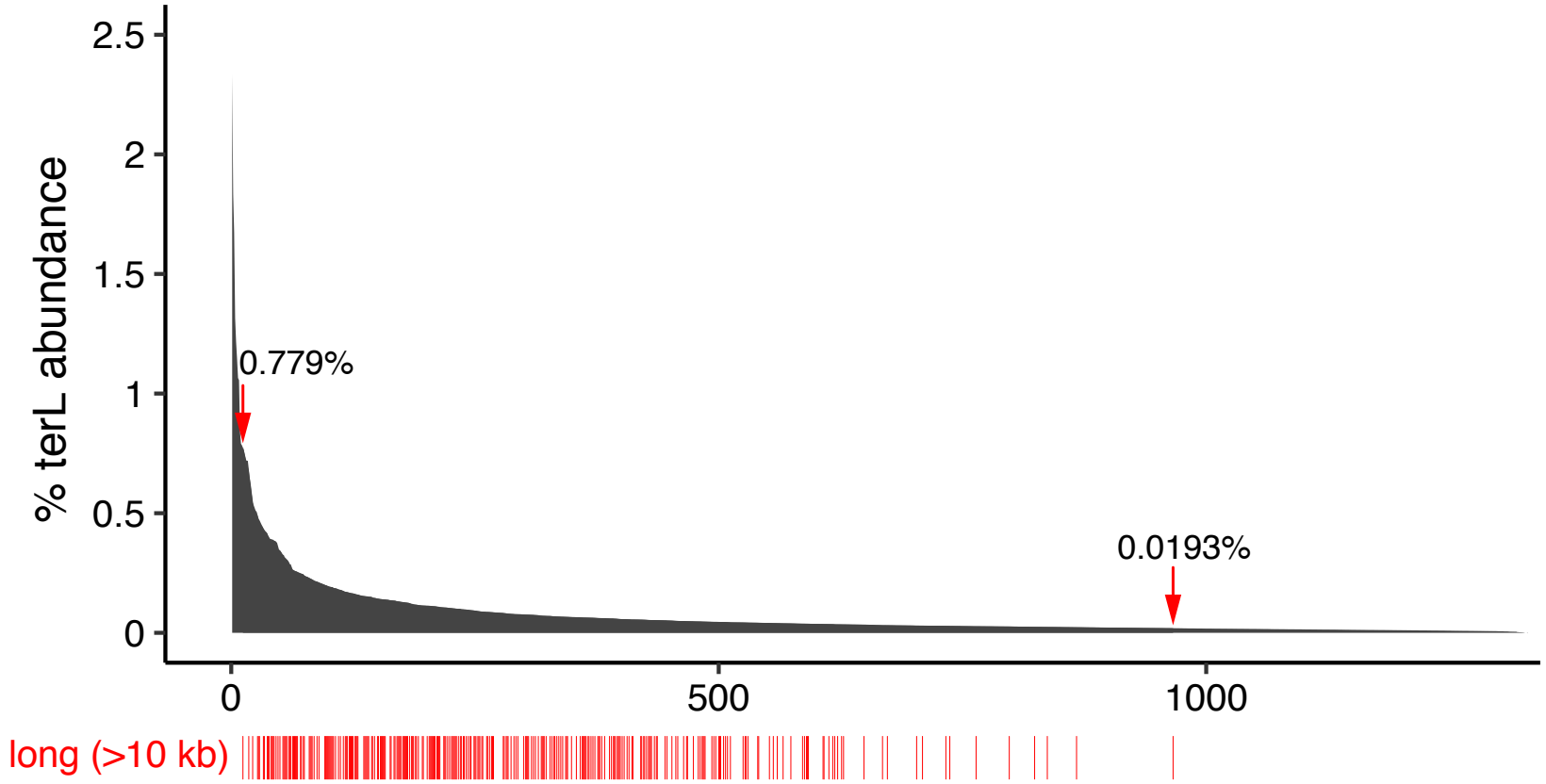

Figure S1 | Virome abundance of OBV long contigs as assessed by putative *terL* genes. Abundance of 297 OBV long contigs (indicated by red ticks) was assessed by the abundance of putative *terL* genes (from 1,330 contigs in total). x-axis represents rank of the contigs. y-axis represents the percentage of *terL* FPKM (average of nine OBV samples). Red arrows indicate two long contigs with the highest and lowest abundance.

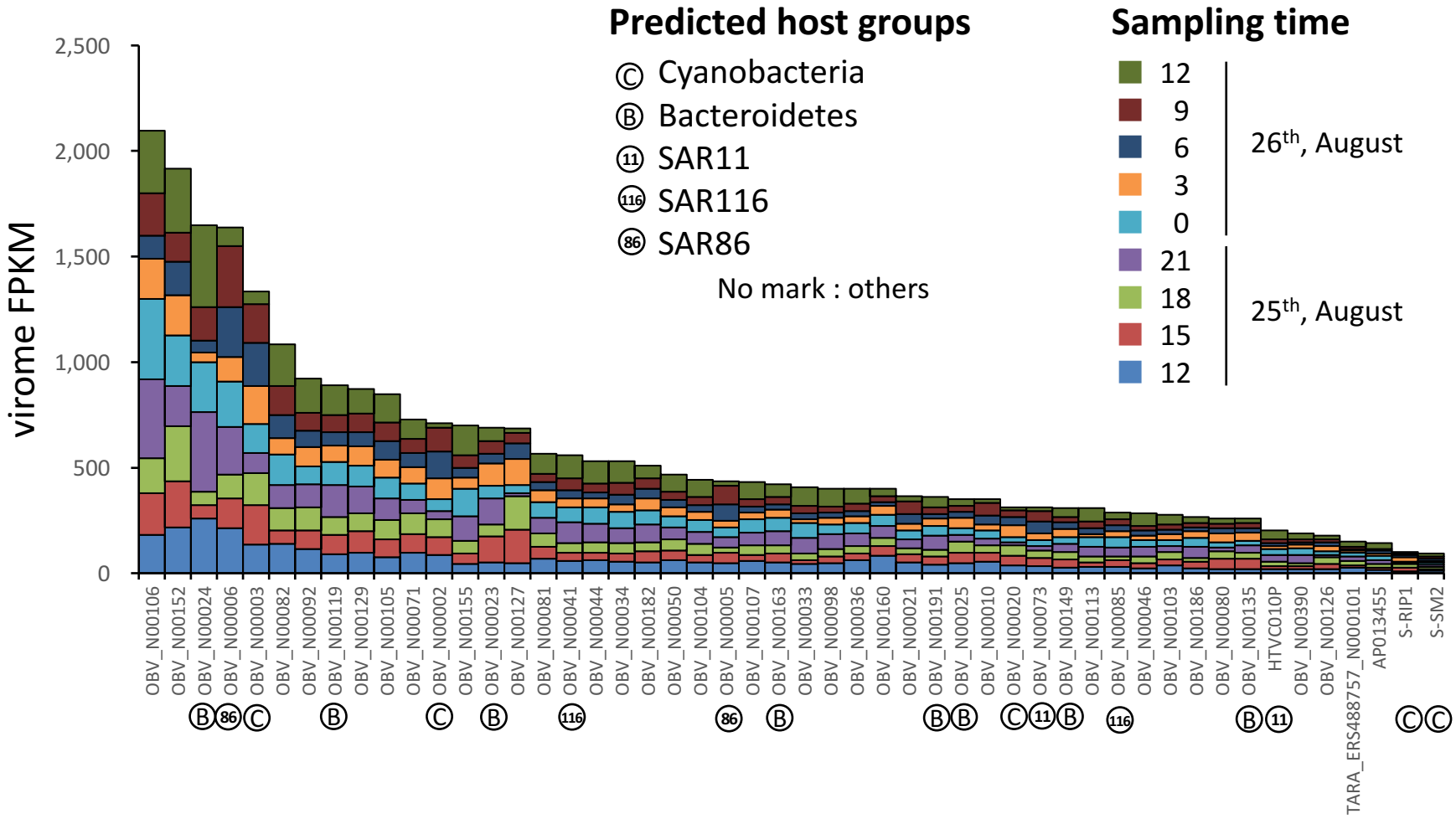

Figure S2 | Ranked virome abundance of complete viral genomes. The 50 most abundant complete viral genomes in nine OBV samples are shown. y-axis represents nine virome FPKM values (sampling time is color coded as shown in the legend). Enclosed characters under the viral genomes indicate predicted host groups as shown in the legend. Sequence ids that begin with 'OBV' are circularly assembled contigs obtained from OBVs. TARA_ERS488757_N000101 and AP013455 are EVGs. HTVC010P: *Pelagibacter* phage HTVC010P. S-RIP1: *Synechococcus* phage S-RIP1, S-SM2: *Synechococcus* phage S-SM2.

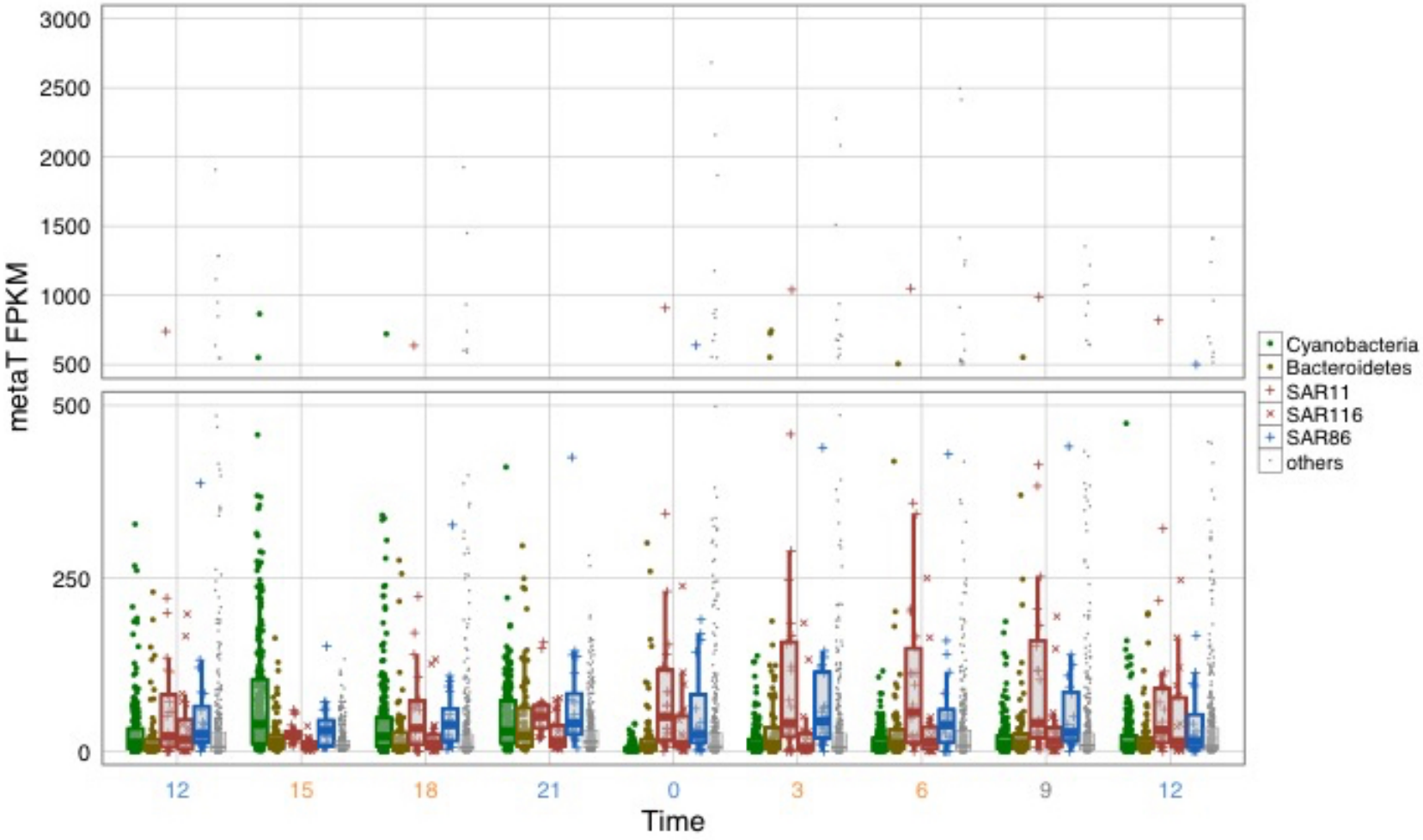

Figure S3 | Transcriptomic abundance changes across nine time points. Transcriptomic abundances of viruses (878 OBV viral contigs) observed in nine samples are shown. The y-axis has a break at the FPKM value of 500. Colors of x-axis labels represent sample groups (blue: oceanic, orange: coastal, gray: mixed; see also Results and Discussion). Predicted host groups are indicated in the figure insert. The boxes represent the first quartile, median, and third quartile. metaT: metatranscriptome. under the viral genomes indicate predicted host groups as shown in the legend. Sequence ids that begin with 'OBV' are circularly assembled contigs obtained from OBVs. TARA_ERS488757_N000101 and AP013455 are EVGs. HTVC010P: *Pelagibacter* phage HTVC010P. S-RIP1: *Synechococcus* phage S-RIP1, S-SM2: *Synechococcus* phage S-SM2.

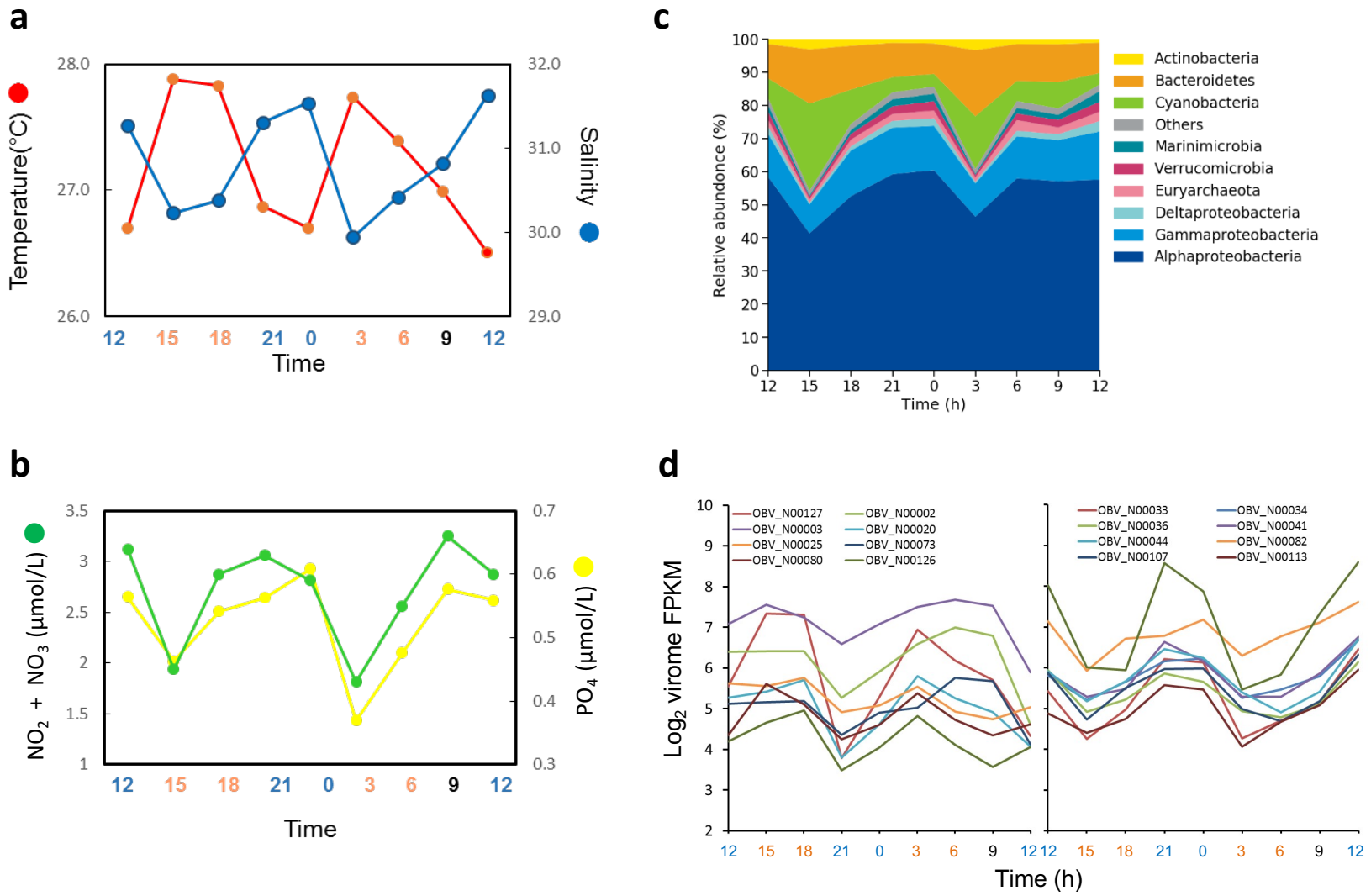

Figure S4 | Changes in environmental parameters, prokaryotic communities, and virome communities across nine time points. (**a**) temperature and salinity; (**b**) concentration of nitrate/nitrite-nitrogen and phosphate-phosphorus; (**c**) prokaryotic communities; (**d**) virome communities. Patterns of virome abundance changes were grouped into seven clusters of temporal dynamics. Two of these clusters, the profiles of which correlated to water mass movements, are shown. For (**a**), (**b**), and, (**d**), the colors of the x-axis labels represent the sample groups (blue: oceanic, orange: coastal, black: mixed).

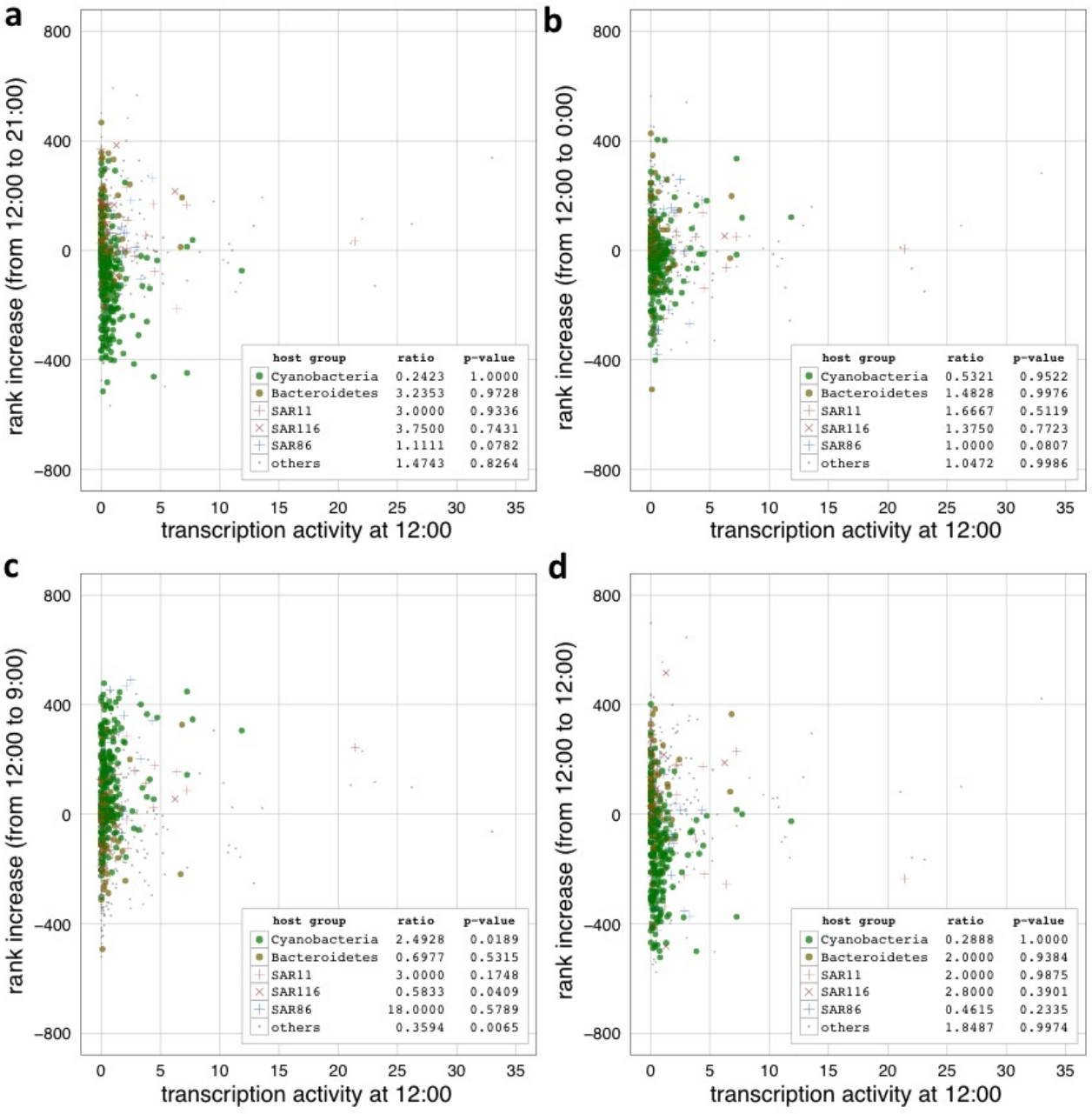

Figure S5 | Infection dependent rank increases in virome abundance for all pairs of time points. As shown in Figure 3b-d, the relationships between transcription activities (i.e., metatranscriptome FPKM divided by virome FPKM) at the first time point and abundance rank increases from the first time point to the second time point for each virus are shown. Statistical analyses and plots were performed on OBV viral genomes whose FPKM values in the virome at the first time point were more than 10.

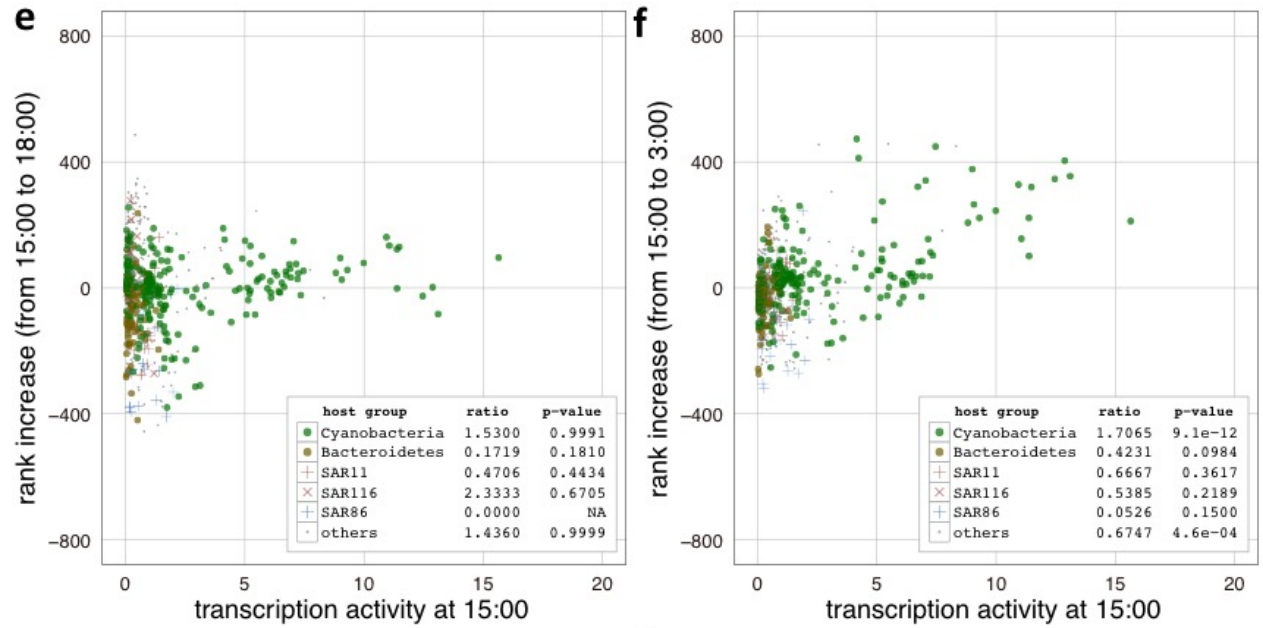

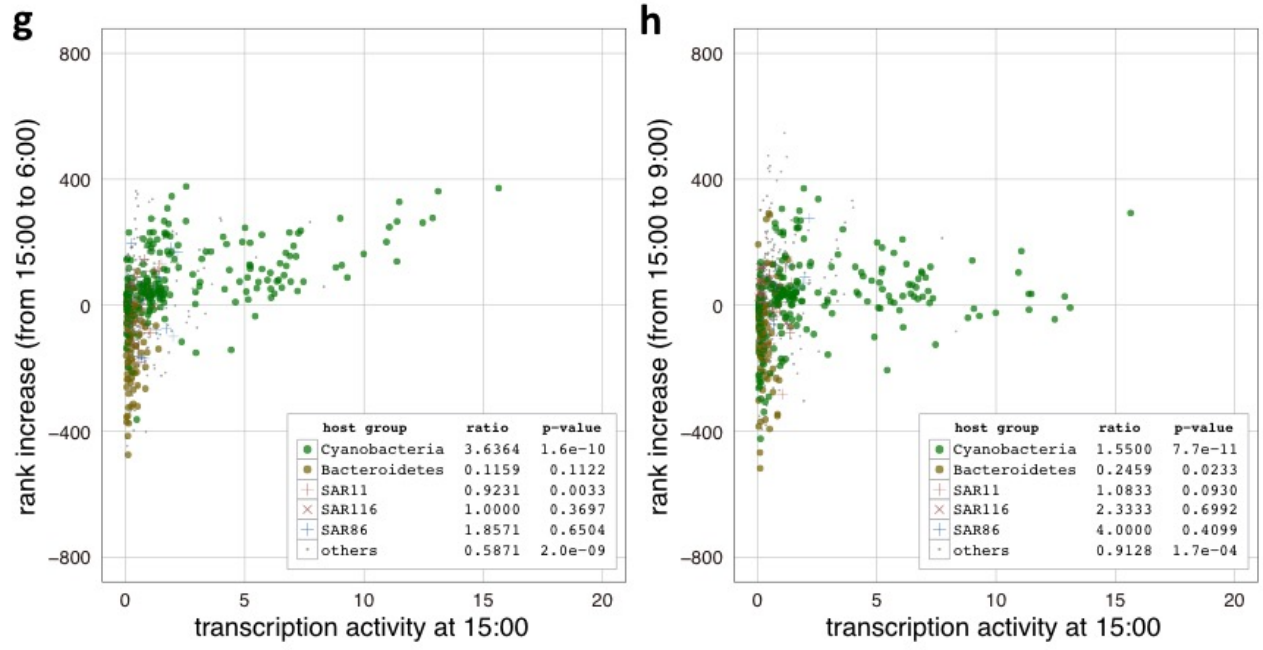

Figure S5 *continued*.

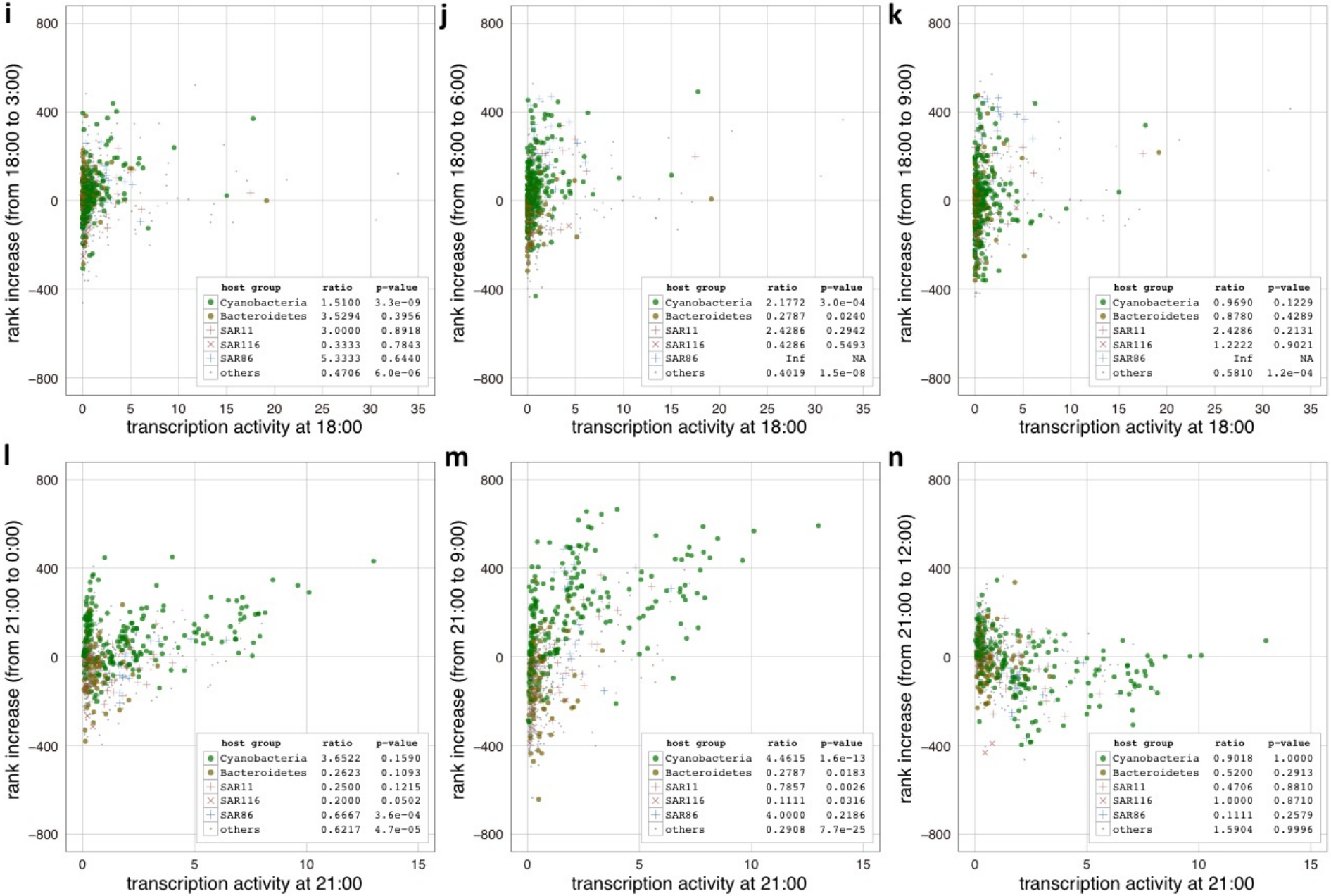

Figure S5 *continued*.

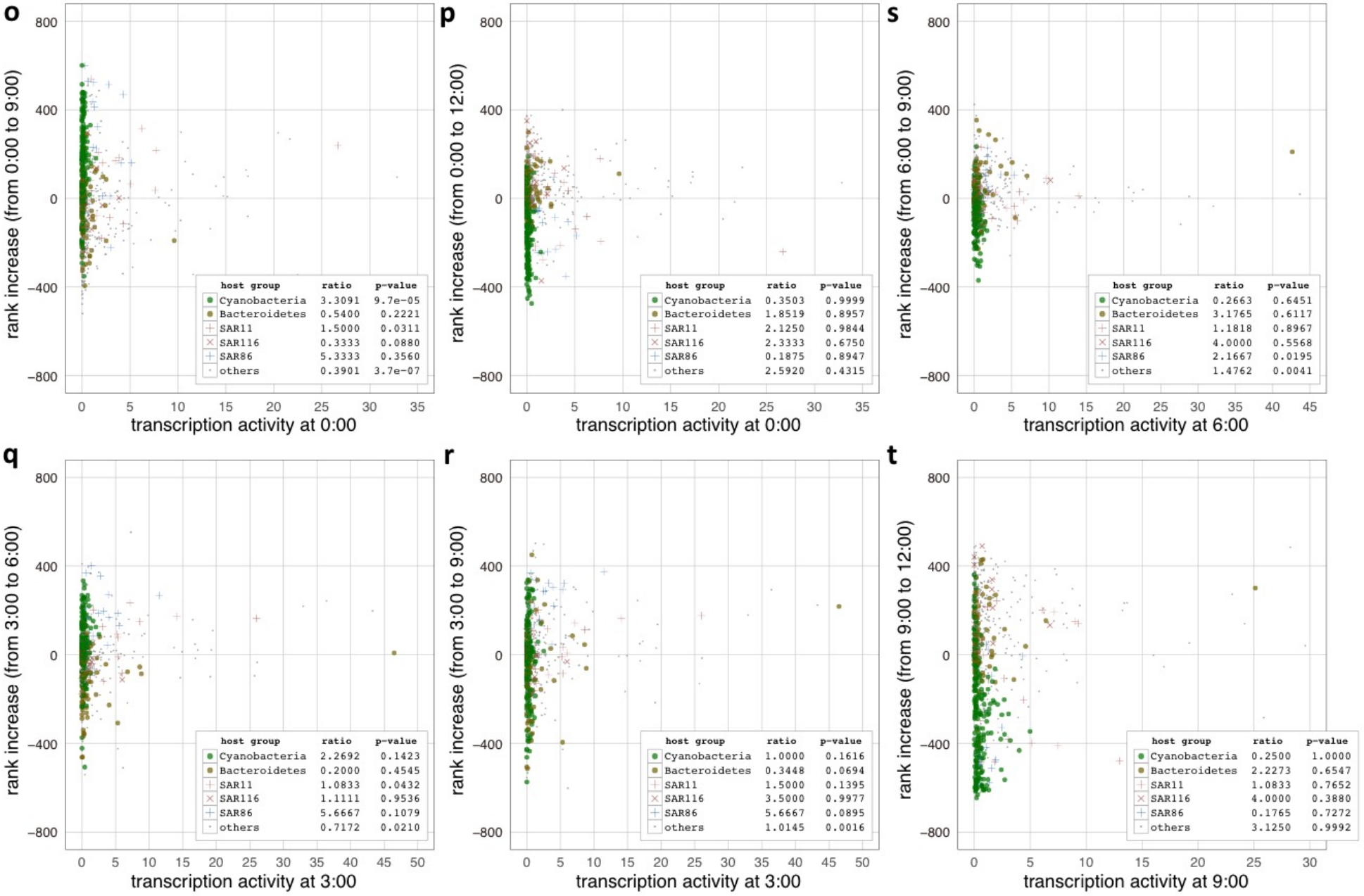

Figure S5 *continued*.